The Journal of Neuroscience, January 1995, 15(1): 574–583

An Anti-CD9 Monoclonal Antibody Promotes Adhesion and Induces Proliferation of Schwann Cells *in vitro*

Michael Hadjiargyrou and Paul H. Patterson

Division of Biology, 216-76, California Institute of Technology, Pasadena, California 91125

We have recently found that CD9, a cell surface glycoprotein involved in intercellular signaling in hematopoietic cells, is also expressed by neurons and glia in the peripheral nervous system. Antibody perturbation experiments were conducted to examine the function of CD9 in neural cells. Three anti-CD9 monoclonal antibodies (mAbs) (ROCA1, ROCA2, B2C11) were tested for their ability to promote adhesion of several Schwann cell lines (S-16, RN22, JS1), primary Schwann cells and PC12 cells. Only B2C11 promotes adhesion in all cells tested. Although ROCA2 immunolabels living cells strongly, it had no effect on the adhesion of any of these cells. In addition, ROCA1 and several positive-staining, control mAbs also had no effect. Another mAb, 192-IgG, directed against the low affinity NGF receptor, also promotes the adhesion of S-16, PC12, and primary Schwann cells. In addition to adhesion, contact of S-16 Schwann cells with B2C11 specifically induces morphological changes and robust proliferation. None of the other mAbs, including 192-IgG, induce proliferation of S-16 cells. These results provide evidence that CD9 may be involved in signaling, activation and growth regulation of cells in the nervous system.

[Key words: CD9, Schwann cells, adhesion, proliferation, monoclonal antibody]

CD9 is a 24–27 kDa cell surface glycoprotein expressed at high levels on the surfaces of developing B-lymphocytes, platelets, eosinophils, basophils, stimulated T-lymphocytes and certain neuroblastoma cell lines (Kersey et al., 1981; Jones et al., 1982; Kemshead et al., 1982; Komada et al., 1983; Boucheix et al., 1987; Boucheix and Benoit, 1988; Von dem Borne et al., 1989). This protein is a member of the "tetraspan" family of four transmembrane domain-containing proteins that are thought to be involved in the regulation of cell growth (Gil et al., 1992). Other members of this family are described in an accompanying article (Kaprielian et al., 1994). CD9 was purified from human platelets (Higashihara et al., 1990; Boucheix et al., 1991; Lanza et al., 1991) and its cDNA cloned (Boucheix et al., 1991; Lanza et al., 1991). Other CD9 homologs were cloned from bovine ocular ciliary epithelial cells (Martin-Alonson et al., 1992), monkey kidney (Vero) cells (Mitamura et al., 1992), and from a mouse kidney cDNA library (Rubinstein et al., 1993). In a search for cell membrane molecules expressed in rostrocaudal gradients the PNS, our group identified three mAbs (ROCA1, ROCA2, B2C11) that bind on the surfaces of peripheral glia and neurons (Suzue et al., 1990; Kaprielian and Patterson, 1993; Tole and Patterson, 1993). We have now identified and cloned the antigen for these mAbs as CD9 from rat sciatic nerve (Kaprielian et al., 1994).

Perturbation studies using anti-CD9 mAbs and transfections have been useful in examining the function of CD9 in hematopoietic cells. Anti-CD9 mAbs stimulate fibrin clot retraction by fibroblasts (Azzarone et al., 1985), induce homotypic adhesion in pre-B lymphocytes (Masellis-Smith et al., 1990), inhibit the motility of lung adenocarcinoma cells (Miyake et al., 1991), augment the adherence of neutrophils to endothelial cells (Forsyth, 1991), and elicit phosphatidylinositol turnover, phosphatidylinositol biosynthesis, and protein-tyrosine phosphorylation in human platelets (Yatomi et al., 1993). Transfection of CD9 elevates diphtheria toxin receptors on toxin-sensitive cells (Mitamura et al., 1992), induces hypersensitivity of mouse cells to diphtheria toxin (Brown at al., 1993), and suppresses cell motility in several cell lines (Ikeyama et al., 1993).

Extensive work with human platelets showed that anti-CD9 mAbs induce activation and aggregation, leading to what is termed an adherent phenotype (Jennings et al., 1990; Griffith et al., 1991). Rather than being directly involved in adhesion, it is thought that CD9, together with other proteins, may function in the initiation of signals leading to cell adhesion. For example, an association between CD9 and the integrin GPIIb-IIIa is induced during platelet activation (Slupsky et al., 1989). The finding that platelets from patients with Glanzman's thrombasthenia, which lack this integrin but not CD9, are not activated by anti-CD9 mAbs further indicates that this CD9-GPIIb-IIIa complex is involved in platelet aggregation (Bouchiex et al., 1983; Higashihara et al., 1985; Miller et al., 1986).

Given our localization of CD9 to peripheral neurons and glia (Tole and Patterson 1993; Kaprielian et al., 1994), we asked whether CD9 can mediate adhesion and cell growth in neural cells. We report here that one anti-CD9 mAb, B2C11, promotes adhesion of a number of Schwann cell lines, PC12 cells and primary rat Schwann cells. In addition, this mAb also stimulates proliferation of one of the Schwann cell lines. An accompanying article further demonstrates that another anti-CD9 mAb enhances motility and migration in primary Schwann cells (Anton et al., 1994).

Received Mar. 29, 1994; revised June 13, 1994; accepted July 12, 1994.

We thank Dr. Richard Quarles for the S-16 cells, Dr. David Anderson for the RN22, JS1, and PC12 cells; Doreen McDowell for media preparation; and Drs. Joshua Sanes, Zaven Kaprielian, Karen Allendoerfer; and Kyung-Ok Cho for their constructive comments on the manuscript. This work was supported by an NINDS grant to P.H.P. and an American Heart Association Research Fellowship and an NIH Training Grant fellowship to M.H.

Correspondence should be addressed to Dr. Michael Hadjiargyrou, Division of Biology, 216-76, California Institute of Technology, Pasadena, CA 91125.

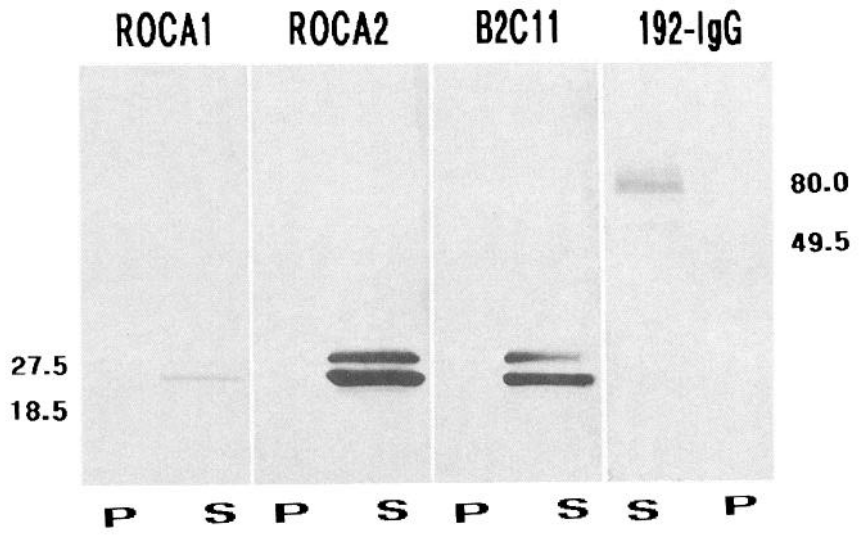

Figure 1. Immunodetection of CD9 and p75 expression in S-16 Schwann cell extracts after immunoblotting of 1% NP-40 supernatant and pellet (*S/P*) fractions. ROCA1, ROCA2, and B2C11 specifically recognize the 26 kDa CD9 band, while the control mAb 192-IgG specifically labels the 75 kDa low affinity NGF receptor. Primary antibody binding was visualized with a peroxidase-conjugated goat anti-mouse IgG secondary antibody. Approximately 100 μg of protein was loaded in each lane.

Materials and Methods

Antibodies. Monoclonal Abs to rat surface proteins, CD9 (ROCA1, ROCA2 and B2C11), p75^{LNGFR} (192-IgG), Thy-1 (OX-7), NGF-inducible large external (NILE) glycoprotein (ASCS4), and a heparan sulfate proteoglycan (pg22) have been previously described (Mason and Williams, 1980; Sweadner, 1983; Akeson and Warren, 1984; Chandler et al., 1984; Matthew et al., 1985; Suzue et al., 1990; Kaprielian and Patterson, 1993; Kaprielian et al., 1994). All of these mouse IgG mAbs were purified from hybridoma supernatants using the mAb Trap-G kit (Pharmacia), and stored at −80°C in a solution containing 1 M glycine-HCl (pH 2.7) and 60 mM Tris-HCl (pH 9) (final pH 7.6).

Cell culture. The rat Schwann cell line, S-16 (Goda et al., 1991), and the rat Schwannomas, RN-22 (Pfeiffer et al., 1978) and JS1 (Kimura et al., 1990), were grown in Dulbecco's modified Eagle's medium (DMEM) supplemented with 10% fetal bovine serum (FBS, Hyclone), glucose (7.5%), L-glutamine (50 mM) and penicillin-streptomycin (50 U/ml and 50 μg/ml, respectively) (GIBCO BRL). The rat pheochromocytoma cell line, PC12 (Greene and Tischler, 1976), was grown on collagen-coated tissue culture plates (10 cm, Falcon) in RPMI 1640 medium supplemented with 10% heat-inactivated horse serum, 5% FBS, as well as glucose, glutamine, and penicillin-streptomycin, as above. All cell lines were maintained at 37°C in a 5% CO_2 humidified incubator.

Primary Schwann cells were isolated by collagenase digestion of neonatal rat sciatic nerve. Nerves were dissected and desheathed from 12 rats and then placed in L-15 air medium (Hawrot and Patterson, 1979) on ice. Nerves were cut into 2 mm pieces, washed in cold Ca^{2+}/Mg^{2+}-free Hanks' solution, and suspended in 2 ml of collagenase (1 mg/ml, Worthington; in Ca^{2+}/Mg^{2+}-free Hanks) that had previously been adjusted to pH 7 with dilute NaOH. Incubation was at 37°C for 60 min, with gentle trituration every 20 min using a fire-polished Pasteur pipette. Cells were washed 2× with L-15 air containing 10% FBS. Undigested tissue was removed by a Falcon cell strainer. The yield was approximately 4 × 10^5 Schwann cells/rat. After a final wash in serum-free medium the cells were treated identically to the S-16 cells for use in the adhesion assay.

Cell adhesion assay. Cells were tested for adhesion to mAbs bound to nitrocellulose in an assay modified from that of (Lotz et al., 1989). Each well of a 96 well plate (Falcon) was coated with 5 liters of a solution of 5 cm^2 nitrocellulose (Schleicher & Schuell, type BA85) dissolved in 6 ml of methanol (Lagenaur and Lemmon, 1987), and allowed to dry for 15 min in a tissue culture hood. Each purified mAb was dissolved at various concentrations in 50 μl of 100 mM carbonate buffer (pH 9.6), and added to the wells. The mAbs were allowed to bind to the nitrocellulose for 1–2 hr at RT followed by two washes with 1× phosphate-buffered saline (PBS). To prevent nonspecific cell binding, the wells were then blocked for 1 hr at 37°C with a 5% BSA solution (in PBS), and afterwards washed 1× with PBS. For the assay, cells were removed from dishes by gently rolling glass beads over the dish, washed in serum-free medium, and resuspended in serum-free medium (DMEM, supplemented with glucose, L-glutamine and penicillin/streptomycin). To generate a single cell suspension, the cells were passed through a cell strainer (Falcon 2350), counted, and added to the test wells at a density of 5–10 × 10^3 cells/well in a volume of 100 μl. The plates were incubated at 37°C for 1–2 hr. At the end of the incubation, each test well was filled with serum-free DMEM and the entire plate was gently covered with an adhesive pressure sensitive film (Falcon 3073). The covered plate was then centrifuged upside-down at 500 rpm for 5 min in a Beckman J-6B centrifuge (with braking) to remove the unbound cells. The adhesive film and most of the excess medium were then removed gently with a multiwell pipetman, leaving behind the adhered cells in 100 μl of DMEM. Adherent cells were assayed by the MTS/PMS assay (Barltrop et al., 1991). Twenty microliters of a solution containing the tetrazolium compound [3-(4,5-dimethylthiazol-2-yl)-5-(3-carboxymethoxyphenyl)-2-(4-sulfophenyl)-2H-tetrazolium, MTS] and an electron coupling reagent (phenazine methosulfate, PMS) (CellTiter 96 AQ_{ueous}, Promega) were added to each well, followed by an incubation of 2–4 hr at 37°C. The optical density at 492 nm was determined with an 96 well plate reader. These data are expressed as the mean O.D. ± SD of triplicate determinations after subtraction of background (no cells added).

Cell proliferation assay. Cell proliferation experiments were conducted in plates identical to those used for adhesion measurements. Once the unbound cells were removed, the plates were further incubated in serum-free medium for 24, 48, or 72 hr. Cell number was then determined using the MTS/PMS solution as described above.

For the micrographs showing cell proliferation in Figure 9, S-16 cells were plated on spots of B2C11 and 192-IgG on 3.5 cm petri dishes (Falcon). These dishes were first coated with the nitrocellulose/methanol solution and air dried for 15 min at RT. In each dish, 250 ng (in 1 μl of PBS) of mAb were dotted in the center and allowed to adsorb for 1–2 hr at RT. The dishes were then washed 2× with PBS and blocked with 5% BSA in PBS for 1 hr at 37°C. Following a wash with PBS, a single-cell suspension of S-16 cells in serum-free DMEM was plated at a density of 1.25 × 10^5 cells/dish for the B2C11-containing dish and 2.5 × 10^5 for the 192-IgG–containing dish. Cells were allowed to adhere for 1.5 hr at 37°C, and unbound cells were removed with two washes of serum-free-DMEM. The same fields were photographed at 2, 24, and 72 hr.

Quantitation of immobilized mAb. To determine how well each mAb used in the perturbation studies adheres to the culture plate, wells were coated with each Ab and the amount of protein was assayed. Duplicate wells of a 96 well plate were coated with 5 μl of a nitrocellulose/methanol solution and allowed to dry for 15 min at RT. Various amounts of each mAb diluted in 50 μl of 100 mM carbonate buffer were added in each well and allowed to adhere for 1–2 hr at RT. The wells were washed 2× with PBS to remove the unbound Ab, followed by the addition of 150 μl of PBS and 150 μl of a 60°C preheated solution of 50:1 Reagent A and B (BCA protein assay, Pierce). The plate was then incubated at 60°C for 1 hr followed by a 15 min cooling period at RT. The optical

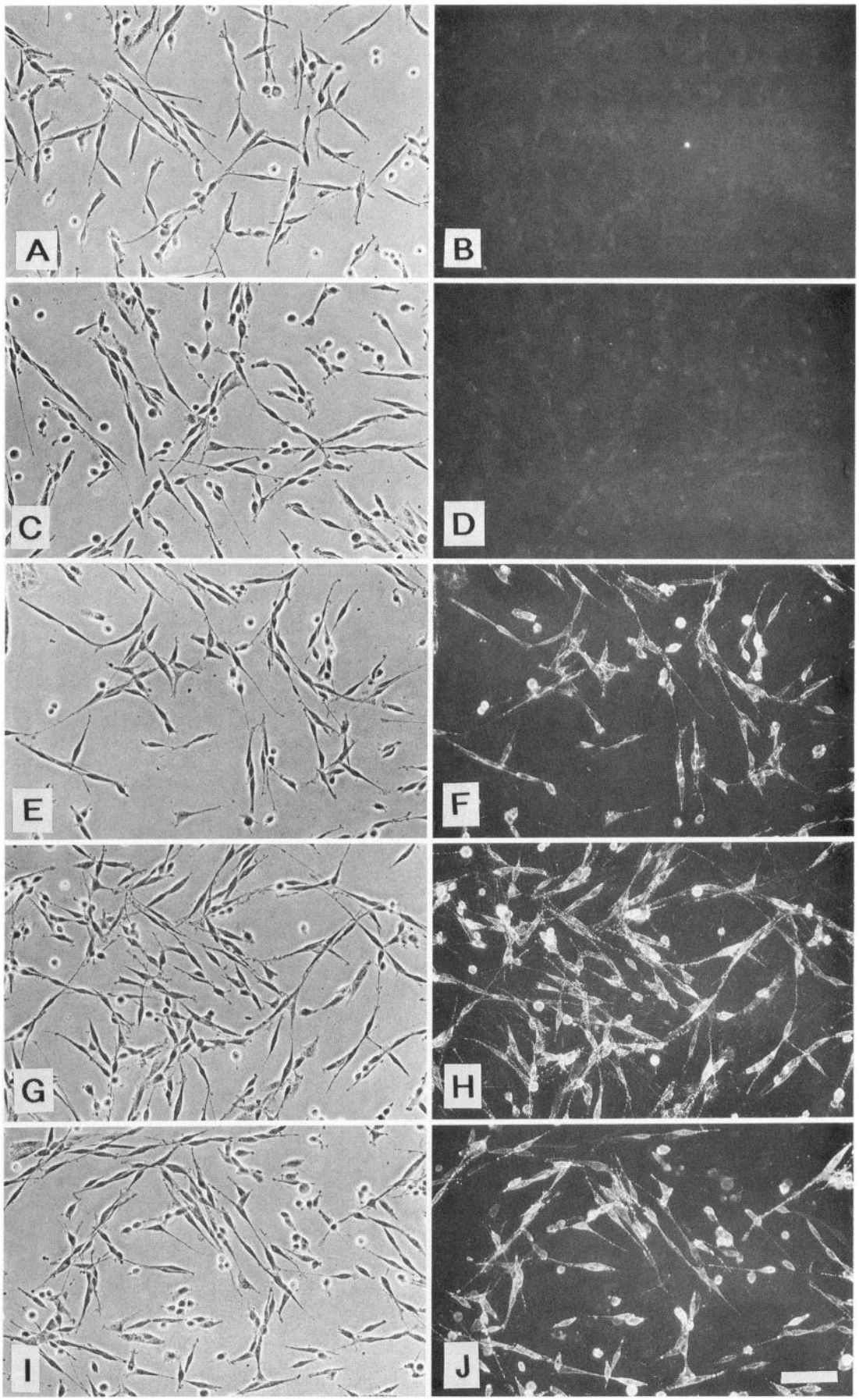
A
B
C
D
E
F
G
H
I
J

density at 570 nm was determined with a 96 well plate reader. The amount of each immobilized Ab was determined by comparing the O.D. obtained with those from wells containing known amounts of mAb. When 0.5 μg, 1 μg, 2.5 μg, and 5 μg was used, 40%, 28%, 16%, and 13%, respectively, was found to adhere on the nitrocellulose/methanol substrate. Very similar results were obtained for all of the mAbs used here.

Immunocytochemistry. S-16 cells were plated on sterile glass coverslips inside a six-well dish (Falcon #3046) and grown for 2–3 d. The cells were then stained for surface antigens with purified mAbs (20 μg/ml) for 45–60 min at RT. Cells were then washed with culture medium and incubated for 30–45 min at RT with fluorescein isothiocyanate (FITC) conjugated goat anti-mouse IgG secondary antibody (Hi-F, Antibodies Inc.) diluted 1:200 in serum-containing culture medium. Cells were then washed 2× with culture medium and fixed with 3% formaldehyde (diluted in serum-containing culture medium) for 10–15 min at RT. Cell-containing coverslips were washed with culture medium and mounted on glass slides in glycerol, containing 8 mg/ml n-propyl gallate (dissolved in 100 mM Tris-HCl, pH 9). Cells were viewed and photographed using an inverted Nikon fluorescence microscope (Diaphot 300).

Protein preparation and immunoblotting. Membrane and cytoskeletal fractions were prepared by homogenization and differential centrifugation, as described previously (Kaprielian and Patterson, 1993). Detergent-soluble and -insoluble fractions were prepared with 1% NP-40 as described previously (Kaprielian and Patterson, 1993), as were SDS-PAGE and immunoblotting procedures.

Results

Expression of CD9 in S-16 Schwann cells

To determine whether CD9 is expressed in S-16 cells, the anti-CD9 mAbs ROCA1, ROCA2, and B2C11 were used for immunoblotting and immunocytochemistry. All three anti-CD9 mAbs detected the 26 kDa CD9 band in detergent-soluble (supernatant) but not insoluble (pellet) membrane fractions (Fig. 1). A second, minor band at 28 kDa, recognized only by ROCA2 and B2C11, represents a glycosylated form of CD9 (Kaprielian and Patterson, 1993). These mAbs do not bind significantly to any other proteins on immunoblots of either detergent-insoluble or soluble fractions. These results are consistent with those obtained previously using ROCA1 and ROCA2 to identify CD9 in membrane extracts of adult sciatic nerve (Kaprielian and Patterson, 1993). As expected, the mAb 192-IgG detected the low affinity NGF receptor, p75, exclusively in the supernatant fraction (Fig. 1).

Expression of CD9 on the cell surface was detected by immunostaining living S-16 cells using the three anti-CD9 mAbs. Strong binding of ROCA2 and B2C11 on the cell bodies and processes of bipolar Schwann cells is illustrated in Figure 2. In contrast, ROCA1 does not detectably bind the surfaces of these cells. In addition, mAb 192-IgG strongly labels the surface of S-16 cells (Fig. 2).

Immobilized antibodies promote adhesion of S-16 cells

Given that anti-CD9 mAbs can induce an adherent phenotype in a variety of hematopoietic cells, it was logical to ask whether the same is true of Schwann cells, which express significant levels of CD9 *in vivo* and *in vitro*. In the first experiments, we tested the ability of various mAbs to enhance S-16 cell adhesion to collagen or fibronectin substrata when the mAbs were added in solution, with and without secondary, goat anti-mouse antibodies. We were unable to demonstrate an effect of the three anti-CD9 mAbs (ROCA1, ROCA2, and B2C11), or two control mAbs, 192-IgG (which labels the surface of S-16 cells, and thus serves as a positive control) and ASCS4 (anti-NILE), (which does not stain these cells, negative control) (data not shown). In a second set of experiments, adhesion assays were conducted with the same mAbs attached to latex beads and covaspheres. S-16 cells were incubated with mAb-coated beads or covaspheres in solution for 1 hr at RT, and then plated on either immobilized fibronectin or tissue culture plastic surfaces. None of the mAb-coated beads or covaspheres influences the rate of S-16 cell binding to these surfaces (data not shown).

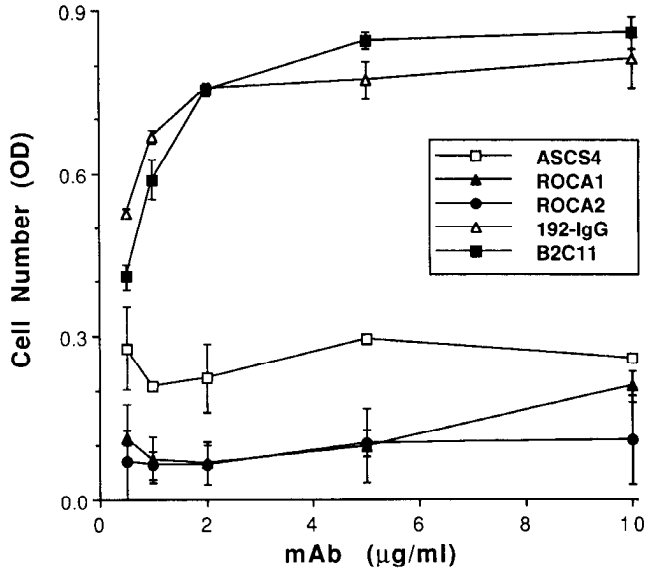

Figure 3. Adhesion of S-16 cells to immobilized mAbs; 1×10^4 cells were added to each well of a 96 well plate containing various concentrations of each mAb that were immobilized on a nitrocellulose substratum. Cells were then exposed to the immobilized mAbs in serum-free medium for 90 min prior to removal of unbound cells by centrifugation. The number of adherent cells was determined spectrophotometrically by the MTS/PMS assay. The entire assay is described in detail in materials and methods. Not shown in graph were the value of cells that adhered on 5% BSA (used as a negative control) which was 0.168 ± 0.033.

In contrast, when these mAbs were tested by immobilizing them on a nitrocellulose-coated dish surface, a striking enhancement of S-16 cell adhesion is observed on two mAbs. As can be seen in Figure 3, B2C11 and 192-IgG both promote adhesion after 90 min of exposure at input mAb concentrations ranging from 0.5–10 μg/ml. Surprisingly, ROCA2 has no effect on cell adhesion, despite its strong immunostaining of the cell surface. The lack of effect of ROCA2 shows that not all immobilized mAbs can influence cell adhesion, and indicates that simple Ab-antigen binding is not sufficient for adhesion at 500 rpm. The ROCA1 and ASCS4 mAbs, which do not label these cells, also have no effect on cell adhesion. The cells that bind to immo-

←

Figure 2. Surface immunofluorescence labeling of CD9 and p75 in S-16 cells. Living cells were incubated with purified mAb (20 μg/ml) and secondary FITC-conjugated, goat anti-mouse IgG secondary Ab, and then fixed as described in Materials and Methods. *A* and *B*, Phase and fluorescent views of cells stained with secondary mAb. *C* and *D*, Phase and fluorescent views of cells stained with ROCA1. *E* and *F*, Phase and fluorescent views of cells stained with ROCA2. *G* and *H*, Phase and fluorescent views of cells stained with B2C11. *I* and *J*, Phase and fluorescent views of cells stained with 192-IgG. Scale bar, 100 μm.

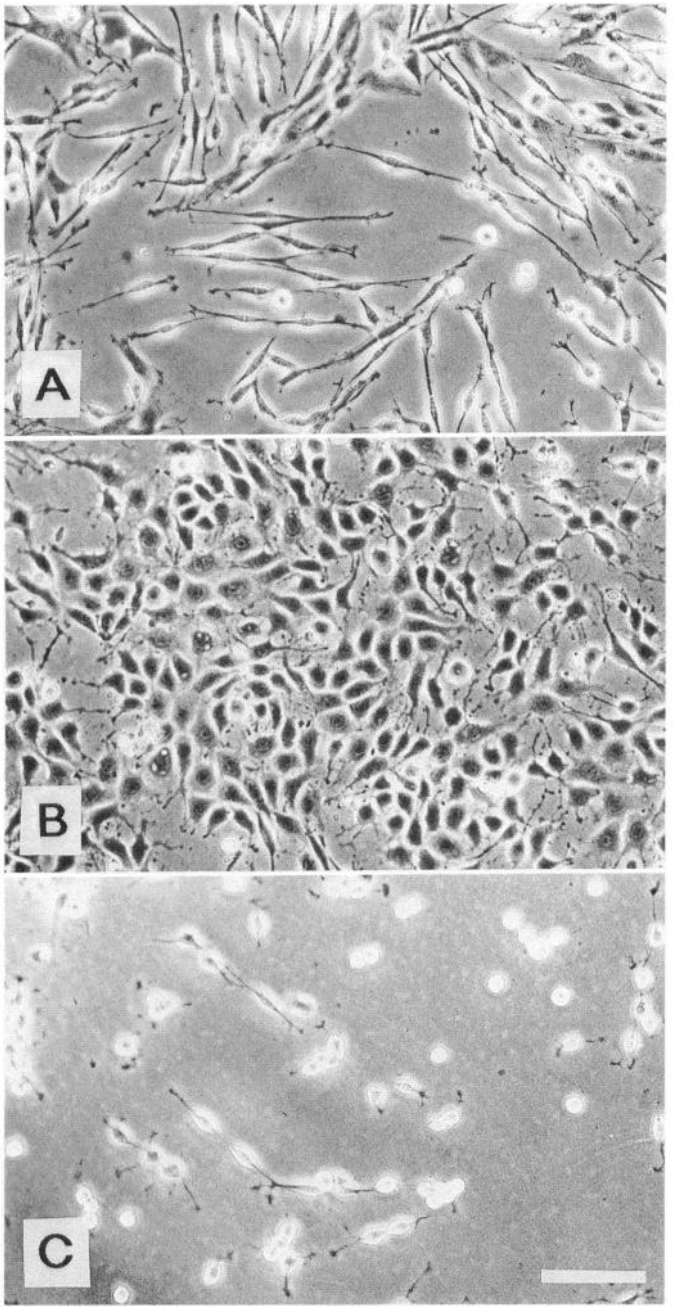

Figure 4. Immobilized B2C11 induces morphological changes in S-16 cells. Cells were exposed for 24 hr to either tissue culture plastic in the presence of serum containing medium (*A*), or 5 μg/ml immobilized B2C11 (*B*) or 192-IgG (*C*), in serum-free medium. Scale bar, 100 μm.

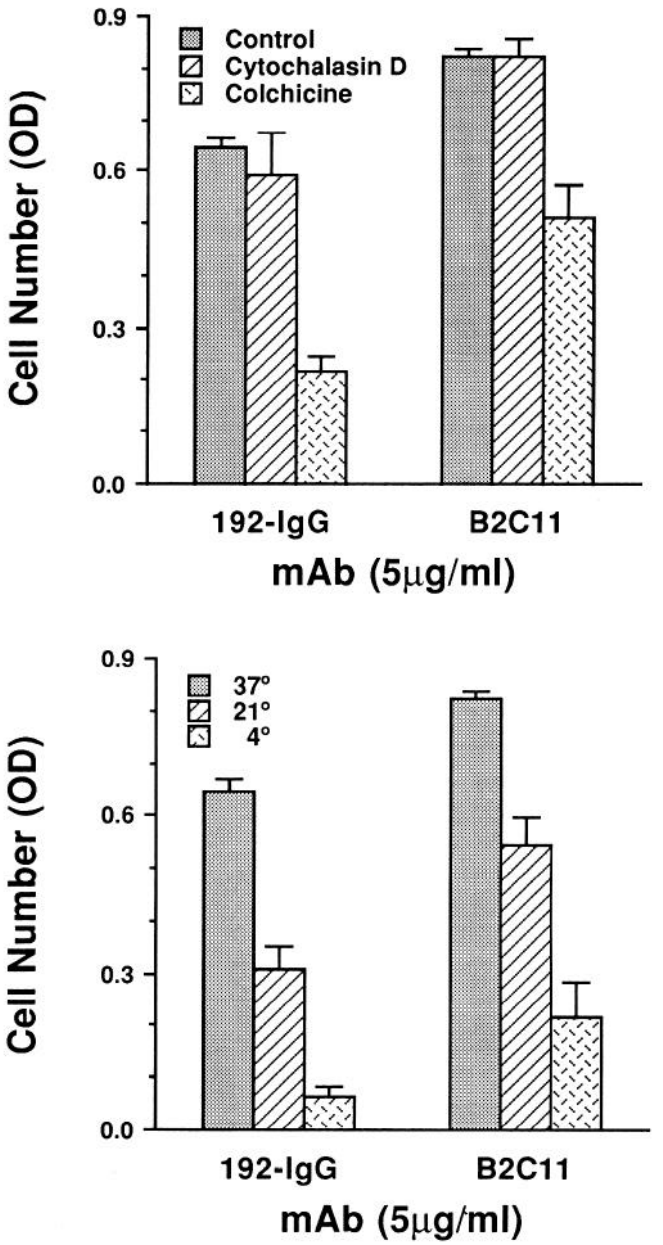

Figure 5. Effects of cytoskeleton-disrupting agents and temperature of S-16 adhesion on immobilized 192-IgG and B2C11; 1.2×10^4 cells were plated on each mAb and allowed to adhere for 90 min in the presence of each agent at 37°C, or at the noted temperature before removal of unbound cells by centrifugation. The number of bound cells was determined spectrophotometrically by the MTS/PMS assay as described in Materials and Methods. Colchicine (10 μM) but not Cytochalasin D (20 μM) disrupts S-16 adhesion on both immobilized mAbs at 37°C. Decreasing the temperature also disrupts S-16 adhesion on both immobilized mAbs.

bilized B2C11 and 192-IgG can be distinguished by their morphology; on B2C11 the cells flatten and spread within the first 30–45 min of contact. As a result, these normally bipolar cells (Fig. 4*a*) resemble flat, polygonal fibroblasts after 24 hr on B2C11 (Fig. 4*b*). Adhesion of S-16 cells to 192-IgG does not induce an obvious morphological transformation; the cells remain rounded or bipolar (Fig. 4*c*).

To determine whether there were any other differences in the adhesion of S-16 cells to immobilized B2C11 and 192-IgG, the rate and strength of cell adhesion to Ab-coated dishes was measured. The rate of adhesion was measured by incubating cells on the mAbs for various times (15, 30, 45, 60, and 90 min) followed by removal of nonadherent cells by centrifugation at 500 rpm (the speed used in the standard adhesion assay). The strength of adhesion was measured by incubating cells for 90 min followed by centrifugation at higher speeds (1000 and 1500 rpm). Results from these experiments indicate that initial binding of S-16 cells to B2C11 occurs more rapidly and is followed by a tighter adhesion in comparison to 192-IgG (data not shown). Another comparison involves measuring the affinity of 192-IgG

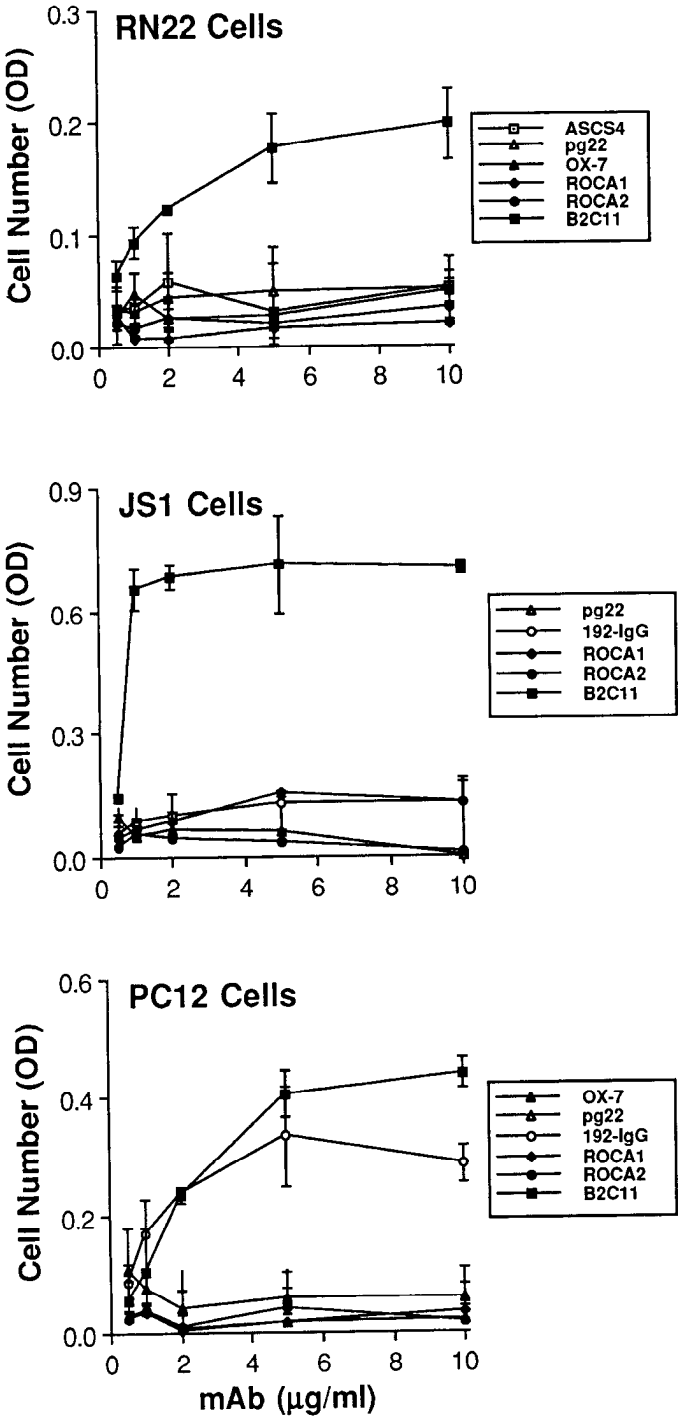

Figure 6. Adhesion of RN22, JS1, and PC12 cells to immobilized mAbs; 1×10^4 RN22 and JS1 cells and 5×10^3 PC12 cells were added to wells containing various concentrations of immobilized mAbs. Cells were then incubated in serum-free medium for 90 min, and unbound cells removed by centrifugation. The number of adherent cells was determined spectrophotometrically by the MTS/PMS assay. Not shown in the graphs are the O.D. numbers of cells adhering to 5% BSA (used as a negative control): 0.036 ± 0.009 for RN22, 0.065 ± 0.013 for JS1, and 0.012 ± 0.038 for PC12 cells.

for p75, and ROCA2 and B2C11 for CD9 using an ELISA with living S-16 cells. In this assay, 192-IgG and B2C11 have a similar affinity for the cells, which is twofold higher than that of ROCA2 for the same cells (data not shown).

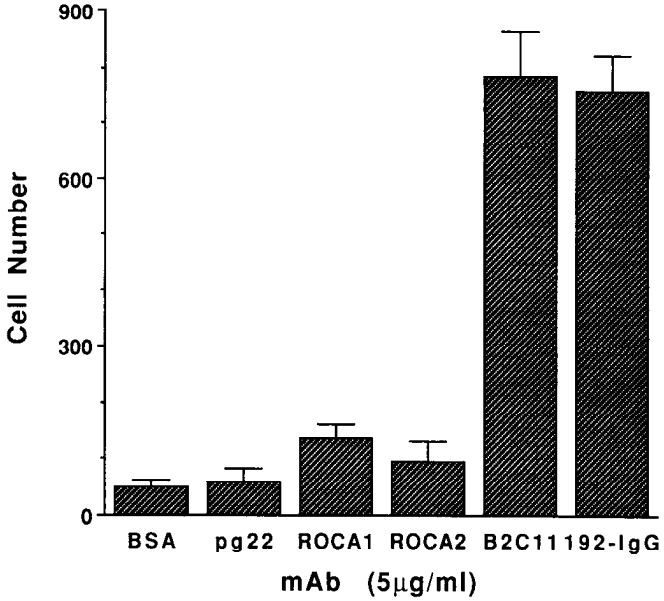

Figure 7. Adhesion of primary Schwann cells to immobilized mAbs; 2×10^4 cells were added to each well of a 96 well plate containing 5 μg/ml of each mAb that was immobilized on a nitrocellulose substratum. Cells were then exposed to the immobilized mAbs in serum-free medium for 90 min prior to removal of unbound cells by centrifugation. Adherent cells were counted visually.

The B2C11-induced morphological changes and strong adhesion of S-16 cells suggest that the cytoskeleton and active cellular energy might be involved. In order to examine this possibility, adhesion assays were carried out at 37°C, in the presence of the microfilament inhibitor, cytochalasin D (20 μM), or the microtubule inhibitor, colchicine (10 μM). As shown by the data in Figure 5, cytochalasin D has no effect on cell adhesion. In contrast, colchicine inhibits adhesion to the B2C11 and 192-IgG surfaces by approximately 32% and 76%, respectively. Similarly, adhesion of S-16 cells to immobilized B2C11 and 192-IgG mAbs is influenced by temperature. S-16 adhesion to both mAbs dramatically decreases as the temperature is lowered from 37°C to 4°C (Fig. 5).

Immobilized antibodies promote adhesion of RN22, JS-1, PC12, and primary Schwann cells

To test the generality of the effects observed with S-16 cells, we tested other glial cell lines derived from peripheral nerve (RN22, JS-1), the sympathetic neuron-like line, PC12, as well as dissociated, primary Schwann cells. In addition to B2C11 and 192-IgG, two other mAbs that also recognize cell surface antigens were used as controls: pg22 (anti-heparan sulfate proteoglycan) and OX-7 (anti-Thy-1). The results of adhesion assays using the rat Schwannoma cell lines, RN22, JS-1, and the adrenal pheochromocytoma, PC12, are illustrated in Figure 6. B2C11 consistently promotes cell adhesion at mAb concentrations of 0.5–10 μg/ml. ROCA2, pg22, and OX-7, mAbs that strongly label these cells (data not shown), do not have any effect on adhesion. As expected, ROCA1 and ASCS4, mAbs that do not label these cells, also have no effect. 192-IgG, however, strongly promotes PC12 cell adhesion (Fig. 6). No morphological changes were observed in the RN22, JS-1, and PC12 cells that adhered to the B2C11 surface.

The ability of these various mAbs to promote cell adhesion

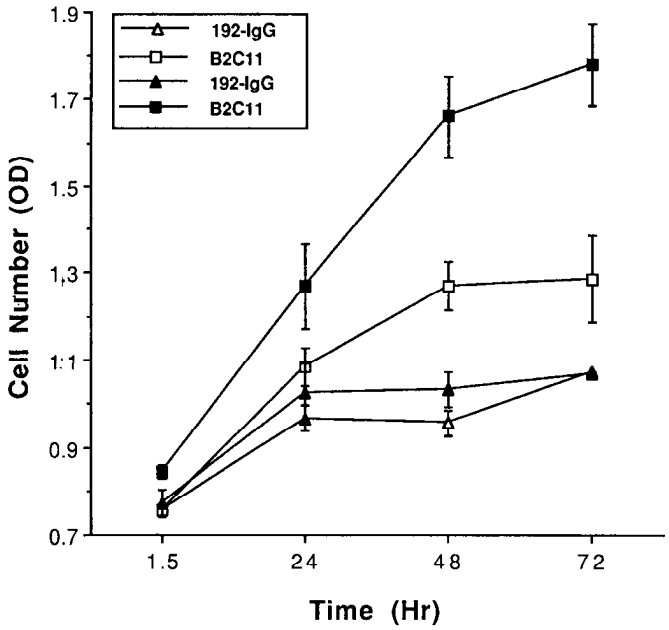

Figure 8. Proliferation of S-16 cells on immobilized B2C11; 2 (*open symbols*) and 5 μg/ml (*solid symbols*) of each mAb was immobilized on a nitrocellulose substratum. Cells (1 × 10^4/well) were then exposed to the immobilized mAbs in serum-free medium for 90 min followed by removal of unbound cells. The number of cells was determined spectrophotometrically by the MTS/PMS assay at 1.5, 24, 48, and 72 hr.

was also tested with primary Schwann cells dissociated from neonatal rat sciatic nerve. Schwann cells were identified on the basis of their expression of both CD9 and $p75^{LNGFR}$, as well as by their characteristic bipolar morphology (data not shown). Results from a 90 min adhesion assay using 5 μg/ml of each mAb are illustrated in Figure 7. A clear enhancement of cell adhesion is seen with B2C11 and 192-IgG. Some flattening of cells on the B2C11 surface was also observed (data not shown).

Immobilized B2C11 stimulates proliferation of S-16 Schwann cells

Another function relevant for the potential signaling role for CD9 and other members of the "tetraspan" family, is growth regulation. Since immobilized B2C11 and 192-IgG promote S-16 cell adhesion, it was possible to compare the ability of these two mAbs to influence cell proliferation. The assay was carried out in serum-free medium lacking any exogenous growth factors or other proteins. Both mAbs were tested at 2 and at 5 μg/ml. Although similar numbers of cells adhere after 90 min to both mAbs, only B2C11 strongly induces S-16 cells to proliferate for the subsequent 72 hr (Fig. 8). Very slight or no growth of S-16 cells results when these cells are plated in serum-free medium on tissue culture plastic in the absence of mAb and monitored for 3 d (data not shown).

The striking nature of this proliferative effect is illustrated in the photomicrographs in Figure 9. In spots of immobilized B2C11 and 192-IgG, defined fields of cells were monitored at 2, 24, and 72 hr. At 2 hr, a few more cells adhere to B2C11 than 192-IgG. By 24 hr, many more flattened cells are present on B2C11. A very clear difference between the cells on these two mAbs appears at 72 hr; a monolayer of flat, polygonal S-16 cells was generated on B2C11, in contrast to the few rounded or bipolar cells present on 192-IgG.

Discussion

CD9 involvement in cell adhesion

In order to begin to examine the potential functions of CD9 in the nervous system, we have carried out antibody perturbation experiments with cultured cells. Adhesion and proliferation assays were conducted with a number of Schwann cell lines (S-16, RN22, and JS1), primary Schwann cells, as well as PC12 cells. The data reveal that B2C11, one of the mAbs against CD9, promotes adhesion of all cells tested. Surprisingly, the $p75^{LNGFR}$ mAb, 192-IgG, also promotes cell adhesion. Both of these adhesive effects where demonstrated only when the mAbs were immobilized on a nitrocellulose substratum. A possible explanation for the immobilization requirement is that this method allows binding to CD9 or p75 at the cell surface without internalization, thus prolonging the ability of the mAb to maintain a sustained activation signal. This hypothesis was also proposed to explain the proliferation of human T4 cells in response to immobilized anti-CD3 mAb (Geppert and Lipsky, 1987). That study also reported that the mAb that stimulates cell proliferation had no effect when presented to cells in soluble form, as was the case in our experiments.

In contrast to the effects displayed by B2C11, the other anti-CD9 mAb, ROCA2, which shows the same affinity to S-16 cells as B2C11 (at 5 μg/ml), showed no effect on adhesion. This result serves as an important control experiment since it suggests that this adhesion assay is not merely measuring Ab-cell binding, but rather a possible sequence of downstream events necessary for adhesion. Simple Ab-cell binding was not sufficient for cell attachment to the nitrocellulose surface after centrifugation at 500 rpm. Since it is known that the two mAbs (ROCA2 and B2C11) recognize distinct epitopes on CD9 (Kaprielian et al., 1994), the effect of B2C11 on cell adhesion and proliferation may depend on stimulation through a particular site on the protein. We speculate that the site recognized by B2C11 is a functional epitope and may be a binding site for a natural ligand of CD9. In this view, B2C11 would mimic the effects of the natural ligand. In contrast, ROCA2 recognizes a nonfunctional epitope and therefore displays no effect. It is possible that the slight difference between ROCA2 and B2C11 in their affinities for CD9 may be responsible for their different activating properties. Differences in affinity, however, will not explain why B2C11 stimulates S-16 cell proliferation while 192-IgG does not. Lastly, the third anti-CD9 mAb, ROCA1, does not immunolabel living cells and does not show any biological effects. We postulate that the ROCA1 epitope is blocked on the surface of cells tested here as it appears to be in Schwann cells in caudal segments of intercostal nerve, satellite cells of caudal sympathetic ganglia and in sciatic nerve (Suzue et al., 1990; Kaprielian and Patterson, 1993). This masking would apply only to intact cells, however; ROCA1 binds to CD9 on immunoblots of all of these cells.

The induction of adhesion by mAb 192-IgG in S-16, PC12 and primary Schwann cells was a surprising finding, since it was not known that the low affinity NGF receptor, p75, could play a role in cell adhesion. It is hypothesized that p75 functions as part of a multimeric complex with the high affinity tyrosine-kinase receptors (*trk* oncogenes) to mediate the actions of the various neurotrophins (reviewed in Barker and Murphy, 1992). Although this may be the primary function of p75, our data suggest that it could also play an indirect role in cell adhesion.

The adhesion of S-16 cells promoted by B2C11 and by 192-

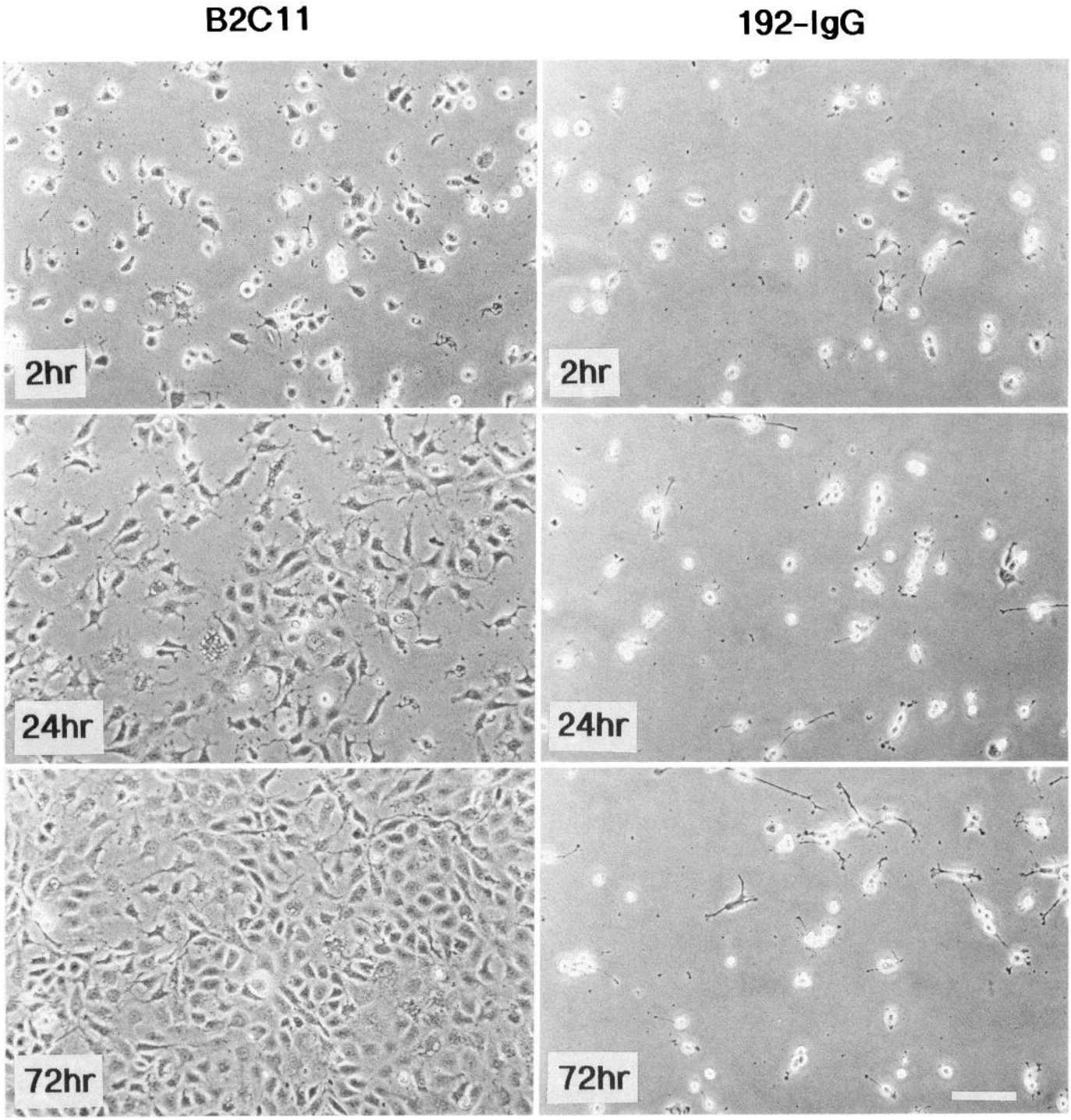

Figure 9. Proliferation of S-16 cells on immobilized B2C11. One microliter of each mAb (250 ng) was dotted in the center of a 33 mm petri dish on a nitrocellulose substratum. Cells were then exposed to the immobilized mAbs for 90 min in serum-free medium prior to removal of unbound cells. The same fields of cells were then photographed at 2, 24, and 72 hr. Scale bar, 100 μm.

IgG is similar in that cells on both mAbs respond in the same way to the various treatments applied here (temperature, cytochalasin D, and colchicine). Binding to B2C11 and 192-IgG can, however, be distinguished by the morphology of the S-16 cells and the rate and strength of adhesion. Contact of S-16 cells with B2C11 (unlike 192-IgG) leads to a rapid and tight adhesion, followed by striking morphological changes. Consequently, these normally bipolar cells resemble flat, polygonal fibroblasts, probably as a result of cytoskeletal protein rearrangements. This notion is supported by previous studies with immobilized mAbs. For example, an immobilized mAb directed against the leukocyte function-associated antigen 1 (LFA-1) causes a human T cell line to develop dendritic processes containing microtubules and intermediate filaments (Kelleher et al., 1990). An immobilized mAb against a novel 20 kDa protein induces both cell adhesion and cytoskeleton-dependent morphological changes

in a number of T cell lines (Lin et al., 1992). These changes include the formation of processes similar to those seen with the anti-LFA-1 mAb.

CD9 involvement in cell growth regulation

Although both 192-IgG and B2C11 promote cell adhesion, only B2C11 strongly induces proliferation of S-16 cells in serum-free medium, indicating that adhesion does not necessarily lead to proliferation. Thus, adhesion and proliferation are separable and can be studied independently in this paradigm. It is noteworthy that the serum-free medium used in these assays was not supplemented with any growth factors or other proteins. We speculate that the capability of S-16 cells to survive and grow under these conditions is due to CD9-stimulated production and release of an autocrine growth factor(s). This hypothesis is supported by the demonstration that both normal and immortalized Schwann cells can secrete an autocrine growth factor that is effective in stimulating their proliferation (Porter et al., 1987). In addition, it is well established that normal and immortalized Schwann cells produce platelet-derived growth factor B-chain, brain-derived neurotrophic factor, Schwannoma-derived growth factor, ciliary neurotrophic factor, NGF (reviewed in Eccleston, 1992; LoPachin and Aschner, 1993; Reynolds and Woolf, 1993).

Support for our finding that CD9 is involved in proliferation of Schwann cells comes from previous perturbation experiments implicating other members of the tetraspan family (Gil et al., 1992) in cell growth regulation. For example, mAbs against CD37, a human B-lymphocyte–associated antigen, enhance the mitogenic effect of anti-immunoglobulin antibodies on B cells but inhibit activation induced by anti-CD20 mAbs and B-cell growth factor on the same cells (Ledbetter et al., 1987). Moreover, a mAb against TAPA-1, a lymphoid cell surface antigen, induces antiproliferative effects on numerous human lymphoid cell lines (Oren et al., 1990). More recently, a mAb against OX-44 (the rat homologue of human CD53) was found to be mitogenic for primary rat splenic T cells (Bell et al., 1992). Lastly, ME491, a melanoma-associated antigen that is expressed strongly during the early stages of tumor progression, has been suggested to serve as a rapid growth inhibitory protein (Hotta et al., 1988).

In addition to the data on Schwann cell adhesion and proliferation presented in this article, Anton et al. (1994) provide evidence for CD9 involvement in Schwann cell migration. Taken together, these results suggest that CD9 is a multifunctional molecule, implicated in a variety of Schwann cell functions *in vitro*. We hypothesize that B2C11 mimics a natural ligand of CD9, and upon binding, exerts its effects by inducing activation signals, likely candidates being increased Ca^{2+} concentration and protein phosphorylation (Anton et al., 1994). Since CD9 protein and mRNA are expressed by peripheral neurons and glia *in situ* (Tole and Patterson, 1993; Kaprielian et al., 1994), it is possible that CD9 is a regulator of migration, adhesion, and/or growth control *in vivo*.

References

Akeson R, Warren SL (1984) Detection of a cell surface antigen found on rat peripheral nervous system neurons and multiple glia: astrocytes, oligodendrocytes, and Schwann cells. J Neurosci Res 12:41–57.

Anton ES, Hadjiargyrou M, Patterson PH, Matthew WD (1995) CD9 plays a role in Schwann cell migration *in vitro*. J Neurosci 15:584–595.

Azzarone B, Krief P, Soria J, Bouchiex C (1985) Modulation of fibroblast-induced clot retraction by calcium channel blocking drugs and the monoclonal antibody ALB_6. J Cell Physiol 125:420–426.

Barker PA, Murphy RA (1992) The nerve growth factor receptor: a multicomponent system that mediates the actions of the neurotrophin family of proteins. Mol Cell Biochem 110:1–15.

Barltrop JA, Owen TC, Cory AH, Cory JG (1991) 5-(3-Carboxymethoxyphenyl)-2-(4,5-dimethylthiazolyl)-3-(4-sulfophenyl) tetrazolium, inner salt (MTS) and related analogs of 3-(4,5-dimethylthiazolyl)-2,5-diphenyltetrazolium bromide (MTT) reducing to purple water-soluble formazans as cell-viability indicators. Bioorg Med Chem Lett 1:611–614.

Bell GM, Seaman WE, Niemi EC, Imboden JB (1992) The OX-44 molecule couples to signaling pathways and is associated with CD2 on rat T lymphocytes and a natural killer cell line. J Exp Med 175: 527–536.

Boucheix C, Benoit P (1988) CD9 antigen: will platelet physiology help to explain the function of a surface molecule during hematopoietic differentiation? Nouv Rev Fr Hematol 30:201–202.

Boucheix C, Soria C, Mirshahi M, Soria J, Perrot J-Y, Fournier N, Billard M, Rosenfeld N (1983) Characteristics of platelet aggregation induced by the monoclonal antibody ALB_6 (acute lymphoblastic leukemia antigen p 24). Inhibition of aggregation by ALB_6Fab. FEBS Lett 161:289–295.

Boucheix C, Benoit P, Krief P, Billard M, Mishal Z, Azzarone B, Rendu E, Esnouf J, Bredoux R, Levy-Toledano S, Soria C, Perrot JY, Mirshahi M, Giannoni F, Bernadou A, Soria J (1987) Platelet aggregation induced by CD9 mAbs. Mechanisms and comparisons with platelet aggregating properties of mAbs directed against other membrane antigens. In: Platelet aggregation induced by CD9 mAbs. Mechanisms and comparisons with platelet aggregating properties of mAbs directed against other membrane antigens (McMichael AJ, ed), pp 780–782. Oxford: Oxford UP.

Boucheix C, Benoit P, Frachet P, Billard M, Worthington RE, Gagnon J, Uzan G (1991) Molecular cloning of the CD9 antigen. J Biol Chem 266:117–122.

Brown JG, Almond BD, Naglich JG, Eidels L (1993) Hypersensitivity to diphtheria toxin by mouse cells expressing both diphtheria toxin receptor and CD9 antigen. Proc Natl Acad Sci USA 90:8184–8188.

Chandler CE, Parsons LM, Hosang M, Shooter EM (1984) A monoclonal antibody modulates the interaction of nerve growth factor with PC12 cells. J Biol Chem 259:6882–6889.

Eccleston PA (1992) Regulation of Schwann cell proliferation: mechanisms involved in peripheral nerve development. Exp Cell Res 199: 1–9.

Forsyth KD (1991) Anti-CD9 antibodies augment neutrophil adherence to endothelium. Immunology 72:292–296.

Geppert TD, Lipsky PE (1987) Accessory cell independent proliferation of human T4 cells stimulated by immobilized monoclonal antibodies to CD3. J Immunol 138:1660–1666.

Gil ML, Vita N, Lebel-Binay S, Miloux B, Chalon P, Kaghad M, Marchiol-Fournigault M, Conjeaud H, Caput D, Ferrara P, Fradelizi D, Quillet-Mary A (1992) A member of the tetraspans transmembrane protein superfamily is recognized by a monoclonal antibody raised against an HLA class I-deficient, lymphokine-activated killer-susceptible, B lymphocyte line. Cloning and preliminary functional studies. J Immunol 148:2826–2833.

Goda S, Hammer J, Kobiler D, Quarles RH (1991) Expression of the myelin-associated glycoprotein in cultures of immortalized Schwann cells. J Neurochem 56:1354–1361.

Greene LA, Tischler AS (1976) Establishment of a noradrenergic clonal line of rat adrenal pheochromocytoma cells which respond to nerve growth factor. Proc Natl Acad Sci USA 73:2424–2428.

Griffith L, Slupsky J, Seehafer J, Boshkov L, Shaw ARE (1991) Platelet activation by immobilized monoclonal antibody: evidence for a CD9 proximal signal. Blood 78:1753–1759.

Hawrot E, Patterson PH (1979) Long-term culture of dissociated sympathetic neurons. In: Long-term culture of dissociated sympathetic neurons (Jakoby WB, Pastan IH, eds), pp 574–583. San Diego: Academic.

Higashara M, Takahata K, Yatomi Y, Nakahara K, Kurokawa K (1990) Purification and partial characterization of CD9 antigen of human platelets. FEBS Lett 264:270–274.

Higashihara M, Maeda H, Shibata Y, Kume S, Ohashi T (1985) A monoclonal anti-human platelet antibody: a new platelet aggregating substance. Blood 65:382–391.

Hotta H, Ross AH, Huebner K, Isobe M, Wendenborn S, Chao MV, Ricciardi RP, Tsujimoto Y, Croce CM, Koprowski H (1988) Molecular cloning and characterization of an antigen associated with early stages of melanoma tumor progression. Cancer Res 48:2955–2962.

Ikeyama S, Koyama M, Yamaoko M, Sasada R, Miyake M (1993) Suppression of cell motility and metastasis by transfection with human motility-related protein (MRP-1/CD9) DNA. J Exp Med 177: 1231–1237.

Jennings LK, Fox CF, Kouns WC, McKay CP, Ballou LR, Schultz HE (1990) The activation of human platelets mediated by anti-human platelet p24/CD9 monoclonal antibodies. J Biol Chem 265:3815–3822.

Jones NH, Borowitz MJ, Metzgar RS (1982) Characterization and distribution of a 24,000-molecular weight antigen define by a monoclonal antibody (DU-ALL-I) elicited to common acute lymphoblastic leukemia (cALL) cells. Leuk Res 6:449–460.

Kaprielian Z, Patterson PH (1993) Surface and cytoskeletal markers of rostrocaudal position in the mammalian nervous system. J Neurosci 13:2495–2508.

Kaprielian Z, Cho K-O, Hadjiargyrou M, Patterson PH (1995) CD9, a major platelet cell surface glycoprotein, is a ROCA antigen and is expressed in the nervous system. J Neurosci 15:562–573.

Kelleher D, Murphy A, Derek C (1990) Leukocyte function-associated antigen 1 (LFA-1) is a signaling molecule for cytoskeletal changes in a human T cell line. Eur J Immunol 20:2351–2354.

Kemshead JT, Fritschy J, Asser U, Sutherland R, Greaves MF (1982) Monoclonal antibodies defining markers with apparent selectivity for particular haematopoietic cell types may also detect antigens on cells of neural crest origin. Hybridoma 1:109–123.

Kersey JS, Lebien T, Abramson CS, Sutherland R, Greaves MF (1981) p24: a human leukemia associated and lymphohematopoietic progenitor cell surface structure identified with monoclonal antibody. J Exp Med 153:726–731.

Kimura H, Fischer WH, Schubert D (1990) Structure, expression and function of a schwannoma-derived growth factor. Nature 348:257–260.

Komada Y, Peiper SC, Melvin SL, Metzgar WD, Tarnowski BH, Green AA (1983) A monoclonal antibody (SJ-9A4) to p24 present on alls, neuroblastomas and platelets. I. Characterization and development of a unique radioimmunometric assay. Leuk Res 7:487–498.

Lagenaur C, Lemmon V (1987) An L1-like molecule, the 8D9 antigen is a potent substrate for neurite extension. Proc Natl Acad Sci USA 84:7753–7757.

Lanza F, Wolf D, Fox CF, Kieffer N, Seyer JM, Fried VA, Coughlin SR, Phillips DR, Jennings LK (1991) cDNA cloning and expression of platelet p24/CD9. J Biol Chem 266:10638–10645.

Ledbetter JA, Shu G, Clark EA (1987) Monoclonal antibodies to a new gp40-45 (CD37) B-cell-associated cluster group modulate B-cell proliferation. In: Monoclonal antibodies to a new gp40-45 (CD37) B-cell-associated cluster group modulate B-cell proliferation (McMichael AJ, ed), pp 339–340. Oxford: Oxford UP.

Lin SL, Derr D, Hildreth JEK (1992) A monoclonal antibody against a novel 20-kDa protein induces cell adhesion and cytoskeleton-dependent morphologic changes. J Immunol 149:2549–2559.

LoPachin RM, Aschner M (1993) Contemporary issues in toxicology. Glial–neuronal interactions: relevance to neurotoxic mechanisms. Toxicol Appl Pharmacol 118:141–158.

Lotz MM, Burdsal CA, Erickson HP, McClay DR (1989) Cell adhesion to fibronectin and tenascin: quantitative measurements of initial binding and subsequent strengthening response. J Cell Biol 109:1795–1805.

Martin-Alonso J-M, Hernando N, Ghosh S, Coca-Prados M (1992) Molecular cloning of the bovine CD9 antigen from ocular ciliary epithelial cells. J Biochem 112:63–67.

Mason DW, Williams AF (1980) The kinetics of antibody binding to membrane antigens in solution and at the cell surface. Biochem J 187:1–20.

Masselis-Smith A, Jensen GS, Seehater JG, Slupsky JR, Shaw ARE (1990) Anti-CD9 monoclonal antibodies induce homotypic adhesion of pre-B cell lines by a novel mechanism. J Immunol 144:1607–1613.

Matthew WD, Greenspan RJ, Lander AD, Reichardt LF (1985) Immunopurification and characterization of a neuronal heparan sulfate proteoglycan. J Neurosci 5:1842–1850.

Miller JL, Kupinski JM, Hustad KO (1986) Characterization of a platelet membrane protein of low molecular weight associated with platelet activation following binding by monoclonal antibody AG-1. Blood 68:743–751.

Mitamura T, Iwamoto R, Umata T, Tomo Y, Urabe I, Tsuneoka M, Mekada E (1992) The 27-kD diphtheria toxin receptor-associated protein (DRAP27) from Vero cells is the monkey homologue of human CD9 antigen: expression of DRAP27 elevates the number of diphtheria toxin receptors on toxin-sensitive cells. J Cell Biol 118: 1389–1399.

Miyake, M, Koyama M, Seno M, Ikeyama S (1991) Identification of the motility-related protein (MRP-1), recognized by monoclonal antibody M31-15, which inhibits cell motility. J Exp Med 174:1347–1354.

Oren R, Takahashi S, Doss C, Levy R, Levy S (1990) TAPA-1, the target of an antiproliferative antibody, defines a new family of transmembrane proteins. Mol Cell Biol 10:4007–4015.

Pfeiffer SE, Betschart B, Cook J, Mancini PE, Morris RJ (1978) Glial cell lines. In: Glial cell lines (Federoff S, Hertz L, eds), pp 287–346. New York: Academic.

Porter S, Glaser L, Bunge RP (1987) Release of autocrine growth factor by primary and immortalized Schwann cells. Proc Natl Acad Sci USA 84:7768–7772.

Reynolds ML, Woolf CJ (1993) Reciprocal Schwann cell–axon interactions. Curr Opin Neurobiol 3:683–693.

Rubinstein E, Billard M, Plaisance S, Prenant M, Boucheix C (1993) Molecular cloning of the mouse equivalent of CD9 antigen. Thromb Res 71:377–383.

Slupsky JR, Seehafer JG, Tang S-C, Masselis-Smith A, Shaw ARE (1989) Evidence that monoclonal antibodies against CD9 antigen induce specific association between CD9 and the platelet glycoprotein IIb-IIIa complex. J Biol Chem 264:12289–12293.

Suzue T, Kaprielian Z, Patterson PH (1990) A monoclonal antibody that defines rostrocaudal gradients in the mammalian nervous system. Neuron 5:421–431.

Sweadner KJ (1983) Post-translational modification and evoked release of two large surface proteins of sympathetic neurons. J Neurosci 3:2504–2517.

Tole S, Patterson PH (1993) Distribution of CD9 in the developing and mature rat nervous system. Dev Dynamics 197:94–106.

Von dem Borne AEGK, Modderman PW, Admiraal LG, Nieuwenhuis HK (1989) Platelet antibodies, the overall results. In: Platelet antibodies, the overall results (Knapp W, Dorken B, Gilks WR, Rieber EP, Schmidt RE, Stein H, Von dem Borne AEGK, eds), pp 951–960. Oxford: Oxford UP.

Yatomi Y, Ozaki Y, Satoh K, Kume S (1993) Anti-CD9 monoclonal antibody elicits staurosporine inhibitable phosphatidylinositol 4,5-biphosphate hydrolysis, phosphatidylinositol 3,4-biphosphate synthesis, and protein-tyrosine phosphorylation in human platelets. FEBS Lett 322:285–290.